HHS Public Access

Author manuscript

Cell Rep. Author manuscript; available in PMC 2023 February 12.

Published in final edited form as:

Cell Rep. 2022 November 08; 41(6): 111615. doi:10.1016/j.celrep.2022.111615.

Curative islet and hematopoietic cell transplantation in diabetic mice without toxic bone marrow conditioning

Charles A. Chang[1,5], **Preksha Bhagchandani**[1,5], **Jessica Poyser**[2], **Brenda J. Velasco**[2], **Weichen Zhao**[1], **Hye-Sook Kwon**[2], **Everett Meyer**[2,3,4], **Judith A. Shizuru**[2,3,4], **Seung K. Kim**[1,3,4,6,*]

[1]Department of Developmental Biology, Stanford University School of Medicine, Stanford, CA 94305, USA

[2]Division of Blood and Marrow Transplantation, Department of Medicine, Stanford University School of Medicine, Stanford, CA 94305, USA

[3]Stanford Diabetes Research Center, Stanford University School of Medicine, Stanford, CA 94305, USA

[4]Northern California JDRF Center of Excellence, Stanford University School of Medicine, Stanford, CA 94305, USA

[5]These authors contributed equally

[6]Lead contact

SUMMARY

Mixed hematopoietic chimerism can promote immune tolerance of donor-matched transplanted tissues, like pancreatic islets. However, adoption of this strategy is limited by the toxicity of standard treatments that enable donor hematopoietic cell engraftment. Here, we address these concerns with a non-myeloablative conditioning regimen that enables hematopoietic chimerism and allograft tolerance across fully mismatched major histocompatibility complex (MHC) barriers. Treatment with an αCD117 antibody, targeting c-Kit, administered with T cell-depleting antibodies and low-dose radiation permits durable multi-lineage chimerism in immunocompetent mice following hematopoietic cell transplant. In diabetic mice, co-transplantation of donor-matched islets and hematopoietic cells durably corrects diabetes without chronic immunosuppression and no appreciable evidence of graft-versus-host disease (GVHD).

*Correspondence: seungkim@stanford.edu.

AUTHOR CONTRIBUTIONS

C.A.C. and P.B. designed and performed experiments, data collection, data analysis, and wrote the manuscript. J.P., B.J.V., and H.-S.K. advised on experimental design and performed experiments, data collection, and data analysis; W.Z. performed experiments and data collection; E.M. and J.A.S. provided guidance and feedback on experimental design and results and reviewed and edited the manuscript. S.K.K. provided guidance and feedback on experimental design and results, wrote the manuscript, supervised the project, and is the guarantor of this work.

DECLARATION OF INTERESTS

J.A.S. is a co-founder, stockholder, and board member and C.A.C. and H.-S.K. are employees and stockholders of Jasper Therapeutics, Inc.

SUPPLEMENTAL INFORMATION

Supplemental information can be found online at https://doi.org/10.1016/j.celrep.2022.111615.

Donor-derived thymic antigen-presenting cells and host-derived peripheral regulatory T cells are likely mediators of allotolerance. These findings provide the foundation for safer bone marrow conditioning and cell transplantation regimens to establish hematopoietic chimerism and islet allograft tolerance.

In brief

Pancreatic islet transplantation in diabetes is limited by requirements for systemic immunosuppression to prevent rejection. Chang et al. report a non-toxic bone marrow conditioning regimen targeting c-Kit that permits stable mixed hematopoietic chimerism across major histocompatibility complex barriers, promoting allotolerance to transplanted islets without systemic immunosuppression and durable diabetes correction.

Graphical Abstract

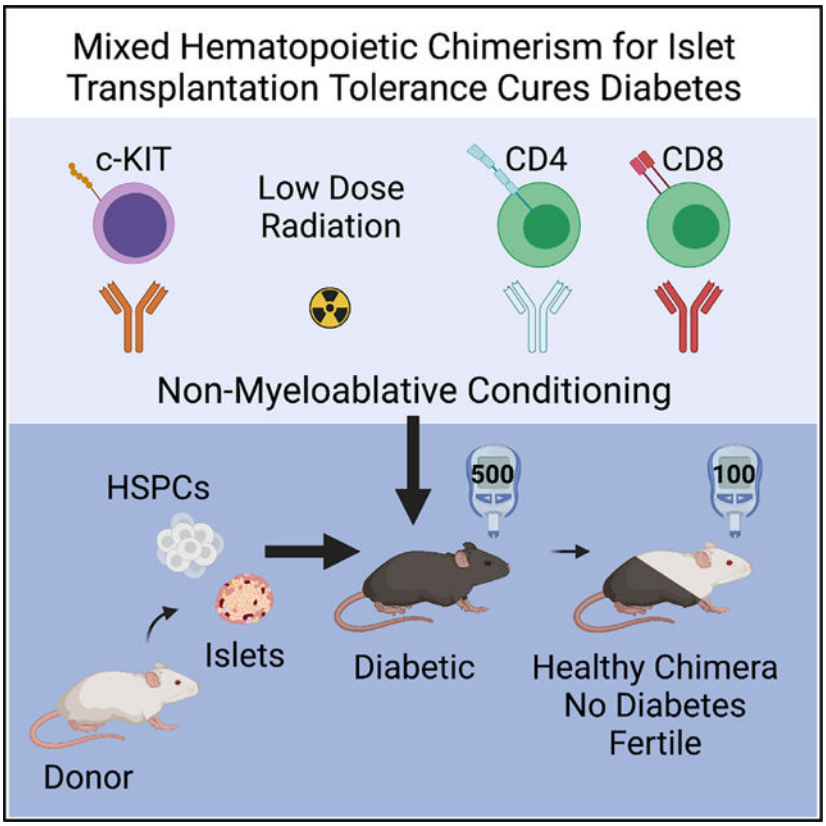

INTRODUCTION

Transplantation of pancreatic islets from major histocompatibility complex (MHC)-mismatched (allogeneic) donors for diabetes after pancreatic β-cell loss is effective but requires chronic immunosuppression to prevent islet rejection (Bartlett et al., 2016; Hering et al., 2016). Standard immunosuppression includes a combination of corticosteroids and T cell inhibitors, but these have diabetogenic and nephrotoxic effects and also increase the risk for opportunistic infections and cancer (Fishman, 2017). Thus, achieving islet

transplantation tolerance without systemic immunosuppression would be a landmark advance (Leventhal and Mathew, 2020; Rickert and Markmann, 2019).

Mixed chimerism, where hematopoietic stem cells (HSCs) of host and donor origin co-exist, is a promising method for achieving durable allotolerance, as demonstrated in solid organ transplantation trials (Busque et al., 2020; Kawai et al., 2008; Leventhal et al., 2012; Messner et al., 2019). Current conditioning regimens that prepare host bone marrow for engraftment by donor HSCs rely on high-dose radiation and/or DNA-damaging chemotherapeutic agents, such as busulfan and melphalan. Such intensive regimens carry risks of severe chronic morbidities (Haghiri et al., 2021; Lee et al., 2013) and are considered too risky for broad application to islet transplantation. However, solely reducing myeloablative agent dosages to mitigate conditioning intensity can result in failure of HSC engraftment (Shaw et al., 2019). Thus, safer non-myeloablative (NMA) conditioning regimens that promote hematopoietic chimerism could advance transplantation tolerance strategies (Bacigalupo et al., 2009). Prior studies of mixed chimerism and islet transplantation have contributed significantly to our understanding of chimerismbased islet allograft tolerance (Pathak and Meyer, 2020). However, these pre-clinical studies incorporated features preventing clinical adoption, including toxic chemotherapeutics for conditioning, reliance on disrupting T cell co-stimulatory pathways such as CD40/CD154, later deemed unsafe in clinical trials, or use of hematopoietic cell preparations that increased graft-versus-host disease (GVHD) risk (Law and Grewal, 2009; Luo et al., 2005; Nikolic et al., 2004; Wang et al., 2014; Xu et al., 2012).

Here, we demonstrate an effective NMA conditioning regimen that permitted mixed chimerism while avoiding these prior limitations. This strategy builds on our previous work showing effective HSC depletion by targeting CD117 (c-Kit), a receptor tyrosine kinase essential for HSC maintenance (Chhabra et al., 2016). Moreover, because of challenges in culturing or preserving primary islets, we developed a simultaneous islet transplantation and hematopoietic cell transplantation (HCT) protocol that approximates a clinically relevant transplantation schedule (Miranda et al., 2013). With this approach, we achieved durable multi-lineage mixed chimerism and islet allograft tolerance, over-coming full MHC barriers, in normal and diabetic mice. These findings provide critical proof of concept for islet tolerance studies and eventual clinical translation for diabetes.

RESULTS

NMA conditioning enables durable multi-lineage mixed donor chimerism

A successful HSC transplantation regimen for achieving islet transplantation tolerance requires eliminating or minimizing genotoxic agents and radiation while using components readily sourced in the clinic. Our conditioning regimen consists of host HSC depletion using an αCD117 monoclonal antibody (mAb) and low-dose total body irradiation (TBI). Induction immunosuppression to prevent acute rejection was achieved through T cell depletion (TCD) using αCD4 and αCD8 mAbs. We tested this regimen in a fully MHC-mismatched transplant setting (Figure 1A) of BALB/c ($H2^d$) donors into B6 CD45.1 ($H2^b$) recipient mice. Recipient B6 mice were given anti-mouse αCD117 mAb (clone ACK2) on day −6 prior to HCT, followed by low-dose TBI on day −3 and TCD on days −2, −1, and 0

(Figure 1B). On day 0, recipients underwent HCT, then were followed for 15 (cohort 1) or 18 weeks (cohort 2).

Four weeks after HCT, we observed robust donor chimerism in all recipient mouse peripheral blood lineages (overall: 65.9% ± 5.7%, $CD3^+$: 16.7% ± 5.6%, $CD11b^+$: 79.2% ± 6.9%, $CD19^+$: 51.4% ± 6.3%; n = 10; Figure 1C). Chimerism was maintained to the experimental endpoint (15–18 weeks) in 9 of 10 recipients (Figures 1D, 1E, S1A, and S1B). Endpoint analysis of the bone marrow (Figure 1F) and spleen (Figure 1G) also revealed robust chimerism, recapitulating observations in peripheral blood. We also confirmed the engraf™ent of donor $Lin^-Sca1^+cKit^+$ (LSK) hematopoietic progenitor cells in host bone marrow (Figure 1F). Importantly, prior studies showed that αCD117 trea™ent or low-dose TBI alone are unable to facilitate robust donor chimerism in immunocompetent models (Czechowicz et al., 2007; Xue et al., 2010). Thus, we established durable mixed chimerism with a marked reduction of conditioning intensity using an NMA regimen targeting CD117.

The general health of mice after conditioning and HCT was assessed by longitudinal body weight measures. In cohort 1 (15 weeks; n = 5), average weight gain from the time of HCT to the end of experiment was 18% ± 3.6% (Figure S2A). In cohort 2 (18 weeks; n = 5), average weight gain was 11.8% ± 9.4% in all but one mouse (Figure S2B). In the mouse that lost weight, necropsy revealed splenomegaly (Figure S2C), possibly reflecting extramedullary hematopoiesis due to cytopenia from delayed bone marrow function. If so, this could be treated in the future with prophylactic HSC growth factors, like in the clinic (Finke and Mertelsmann, 2015). We also observed transient loss of hair pigmentation in a subset of mice (Figure S2D), possibly reflecting CD117 function in hair follicle melanocytes or pigmentation loss from TBI (Aoki et al., 2011, 2013; Czechowicz et al., 2007). Thus, by multiple measures, mice remained healthy after NMA conditioning and achieving mixed chimerism with benign side effects.

Mixed chimerism promotes allogeneic islet tolerance

We investigated if establishment of mixed chimerism between fully MHC-mismatched strains following NMA conditioning promoted donor-matched islet allograft tolerance. To examine both acute immunity and long-term tolerance, islets from sex-matched B6 and BALB/c or third-party FVB ($H2^q$) donors (STAR Methods) were transplanted into mice with mixed chimerism or into conditioned controls (Figures 2A and 2B).

Two weeks after transplantation, BALB/c islet grafts remained intact in mice with mixed BALB/c chimerism with little to no $CD3^+$ T cell infiltration and sparse $CD45^+$ immune cell infiltration (Figure 2C). By contrast, islet grafts from third-party FVB donors were heavily infiltrated by $CD3^+$ and $CD45^+$ cells (Figure 2D). BALB/c grafts were also fully rejected in conditioned nonchimeric controls, as expected (Figure 2E). In islet grafts assessed 14 weeks after transplantation, 100% of both syngeneic B6 (n = 5/5) and donor-matched BALB/c grafts (n = 5/5) remained intact in mice with mixed chimerism (Figure 2F). Thus, mixed hematopoietic chimerism after αCD117 conditioning resulted in acute and long-term donor-matched islet allograft tolerance. Self-tolerance was preserved as demonstrated by engraf™ent of all B6 islet transplants. Rejection of third-party FVB islet allografts demonstrated preserved immunocompetence, including non-self-immunity.

Matched islet transplantation and HCT rescues diabetes in mice

To investigate if combined HCT and islet transplantation could rescue overtly diabetic recipients across the barrier of full MHC mismatch, we used B6 RIP-DTR mice (Bhagchandani et al., 2022). These harbor the *Ins2-HBEGF* transgene and are homozygous for *Ptprc*^{a} (CD45.1). Islet β-cell ablation after a single dose of diphtheria toxin (DT; STAR Methods) renders the mouse insulin deficient and severely diabetic. Male and female B6 RIP-DTR mice were given DT on day −4.5 and made diabetic prior to NMA conditioning. On day 0, conditioned mice received an islet graft from B6, BALB/c, or FVB sex-matched donors and HCT from BALB/csex-matched donors(Figure 3A).Mice were followed for 20 (cohort 1) or 16 weeks (cohort 2) after transplantation.

By 4 weeks after transplantation, all B6 RIP-DTR mice had established multi-lineage mixed chimerism with an overall donor chimerism level of 81% ± 6.2% (n = 11; Figure S3A). This chimerism is slightly higher than in B6 mice (Figure 1C), likely reflecting the increased radiation dose used in B6 RIP-DTR mice. This was durable to the experimental endpoint (16–20 weeks post-transplant) in peripheral blood (Figures 3B, 3C, S3B, and S3C) and bone marrow (Figure 3D). These relatively high levels of donor chimerism suggest that further reductions of conditioning intensity or transplanted HSC dose are possible. Mice that received congenic B6 islets or donor-matched BALB/c islets achieved euglycemia and remained normoglycemic for at least 100 days, and nephrectomy of islet graft-bearing kidneys resulted in a rapid reversion to hyperglycemia in these mice (Figures 3E and 3F). The survival of transplanted B6 and BALB/c islets was confirmed by histology in recovered grafts (Figures 3H and 3I). Assessment of the pancreas in all DT-treated B6 RIP-DTR mice showed few to no remaining islet β-cells (Figure S3D).

FVB islet recipients initially achieved euglycemia but spontaneously reverted to hyperglycemia in a mean of 78 ± 12.9 days (n = 4; Figure 3G). Graft recovery and histological assessment confirmed destruction of transplanted FVB islets (Figure 3J). The duration of FVB graft function exceeded the time frame of islet rejection in normal immunocompetent mice, which is typically 2 weeks (Figure 2). We speculate that this delay reflects a combination of factors, including the transient immunosuppression in graft recipients, time needed for *de novo* effector T cells to mature, and possible effects of resident immune cells in transplanted islets (Zirpel and Roep, 2021). Nevertheless, eventual rejection of third-party islet allografts indicated preservation of immunocompetence in mixed chimeras.

Rescued diabetic mice retain critical functions enhancing life quality

After NMA conditioning, HCT, and islet transplantation in B6 RIP-DTR mice, we measured body weight to assess general health (Figure S4A). By 2 weeks after transplantation, body weight in all mice nadired at 75%–80% of starting weight. Recipients of B6 or BALB/c islets recovered and then stabilized body weight. Mice receiving FVB islets also recovered body weight while euglycemic but rapidly lost weight after reverting to diabetes. Not all mice returned to their starting weight, possibly reflecting limitations of transplanted islet mass in sustaining weight gain. At sacrifice, duodenal histology showed an absence of

GVHD. Intestinal mucosa and glands appeared intact, without evidence of parenchymal inflammation or edema, despite high levels of donor chimerism (Figure S4B).

Standard myeloablative conditioning results in severe morbidities like infertility (Joshi et al., 2014). To test the impact of our NMA regimen on breeding performance, we paired three male B6 RIP-DTR mice, each with diabetes reversal after BALB/c mixed chimerism and islet transplant, with wild-type B6 females. Two of three male mice produced at least two healthy litters each (Figure S4C), while one did not sire any litters. That third male was older (13 vs. 10 months) and heavier (~35 g) compared with the other males (~27 and ~30 g). Age and obesity are known to negatively impact breeding performance (Lecker and Froberg-Fejko, 2016). Thus, islet transplantation and HCT following our NMA regimen reverses diabetes without chronic immunosuppression while preserving fertility.

Regulatory cell subsets delineate mechanisms of immune tolerance

Allotolerance resulting from mixed chimerism has been attributed to a combination of central tolerance, through donor antigen presentation in the thymus leading to deletion of alloreactive T cells, and peripheral tolerance, through the function of regulatory cell types (Beilhack et al., 2003; Zuber and Sykes, 2017). To assess tolerance mechanisms in our model, we characterized CD45.2 donor-derived and CD45.1 host-derived immune cells in the thymus and spleen of BALB/c-B6 RIP-DTR mixed chimeras compared with conditioned controls.

In the thymus, CD45.2 donor-derived dendritic cells (DCs) were present from the three major subsets of $CD11c^+$ DCs including $B220^+PDCA1^+$ plasmacytoid DCs (pDCs), $CD8^+SIRP\alpha^-$ thymus-resident DCs (tDCs), and $CD8^-SIRP\alpha^+$ migratory DCs (mDCs) (Figure 4A). These subsets have been shown to augment negative selection of T cells in the thymus (Audiger et al., 2017; Baba et al., 2009; Hadeiba et al., 2012; Herbin et al., 2016). Negative selection of thymocytes is often accompanied by an increase in thymic regulatory T cell (tTreg) production, and pDCs can promote differentiation of tTregs (Klein et al., 2014). Consistent with this, host $CD4^+$ T cells in mixed chimeras had an increased frequency of tTregs ($CD4^+CD25^{hi}$) compared with conditioned non-chimera controls (6.16% ± 0.85% vs. 3.36% ± 0.63%, respectively; Figure 4B), with host-derived Tregs being the majority contributor (Figure S5A). These results support a mechanism of central tolerance induction in B6 RIP-DTR mixed chimeras, where donor HSCs give rise to DCs capable of antigen presentation in the host thymus to mediate negative selection and augment the generation of host-derived tTregs

Peripheral tolerance in transplantation is associated with Treg activity (Adeegbe et al., 2010). Consistent with our observations in the thymus, we observed increased frequency of splenic Tregs among host $CD4^+$ T cells in mice with mixed chimerism compared with conditioned controls (14.95% ± 2.17% and 5.59% ± 0.79%, respectively; Figure 4C), again with host-derived Tregs being the major contributor (Figure S5B). pDCs were also reported to promote peripheral tolerance by promoting the differentiation of $Helios^-NRP1^+$ peripheral Tregs (pTregs) from conventional T cells (Rogers et al., 2013). We found that mixed chimeras had an increased frequency of splenic pDCs compared with non-chimeras (4.4% ± 0.8% and 1.4% ± 0.3%, respectively; Figure 4D). This effect, however, did not

correlate with a change in the frequency of splenic pTregs, where no difference was observed (Figure S5C). Prior establishment of an immunologically homeostatic state by central tolerance could obviate the need for pTreg expansion. The absence of increased pTregs could also indicate a lack of ongoing inflammation (Chen et al., 2017; Yadav et al., 2013). In summary, durable mixed chimerism and islet tolerance in our models likely reflect both central and peripheral mechanisms that establish and maintain tolerance to donor HSCs and islets.

DISCUSSION

Prior studies show that mixed hematopoietic chimerism can induce donor-specific tolerance, but toxic conditioning regimens and hematopoietic cell preparations previously used have prevented clinical translation (Beilhack et al., 2003; Nikolic et al., 2010; Persaud et al., 2021; Wang et al., 2014). Here, we achieved mixed donor chimerism and durable islet allotolerance after NMA conditioning. Transplantation of donor-matched islets led to diabetes remission without chronic immunosuppression, resulting in excellent functional status. In mice with stable mixed chimerism, we also observed evidence of central and peripheral mechanisms underlying donor-specific tolerance. Advances here chart a pathway toward safer clinical strategies for broader use of islet transplantation in diabetes.

DNA alkylating drugs and high-dose radiation used for HCT conditioning are associated with multiple morbidities, including chronically impaired endocrine function and fertility (Couto-Silva et al., 2001). These complications require extensive counseling and trea™ent (Borgstrom et al., 2020; Wikander et al., 2021). Here, we demonstrated that a small cohort of mice remained fertile and retained good breeding performance following NMA conditioning and diabetes reversal after islet allotransplant and HCT. Further studies with larger male and female cohorts are warranted to assess preservation of quality-of-life metrics after αCD117-based conditioning.

GVHD is a potentially life-threatening complication of HCT and a challenge to expanding HCT use (Flowers and Martin, 2015). Major risk factors for GVHD include the intensity of bone marrow conditioning and HSC source and composition (Czerw et al., 2016; Lazaryan et al., 2016; Nakasone et al., 2015); here, we addressed both risk factors. First, our conditioning regimen is NMA and comparatively mild while retaining high efficacy. Second, we transplanted enriched hematopoietic stem and progenitor cells (HSPCs), depleted of mature effector cells, rather than whole bone marrow (WBM). Clinically, HSPC enrichment is achieved by purifying $CD34^+$ cells using established sorting methods. While HSPC preparations can reduce GVHD risk, they do not engraft as well as WBM due to deficits of immune and other facilitating cells (Huang et al., 2016). We found that NMA conditioning fostered HSPC transplantation to achieve donor chimerism across full MHC barriers and without GVHD.

Allogeneic islet transplantation has been endorsed in the US for type 1 diabetes, but immunosuppression needed to sustain transplanted islets has prevented wider adoption (Pullen, 2021). Here, mixed chimerism and allograft tolerance in a fully MHC-mismatched setting eliminated the need for chronic systemic immunosuppression. All components in

our protocol have equivalent or analogous clinical counterparts, enhancing the promise for clinical translation. For example, human αCD117 Ab (JSP191) is in multi-center trials (ClinicalTrials.gov: NCT02963064, NCT04429191, NCT04784052) and has shown a good safety profile and promising results (Agarwal et al., 2021). Transplant centers experienced with HCT routinely deliver NMA radiation. Our regimen also included anti-T cell therapy to overcome acute immune rejection by the recipients. We used αCD4 and αCD8 Abs for transient TCD, which can also be achieved with anti-thymocyte globulin or other agents with good efficacy and safety profiles. Notably, our mice did not have infectious complications while housed without antibiotic support.

In summary, we have established a translatable NMA conditioning regimen and transplantation protocol to establish mixed hematopoietic chimerism and donor-matched islet tolerance across full MHC barriers, resulting in the reversal of diabetes. These findings motivate investigations to determine if adaptation of our strategy can be used to reverse established autoimmune diabetes or to protect transplanted replacement islet cells derived from renewable sources, including multi-potent stem cell lines.

Study limitations

Our transplantation model was limited to a primary donor strain and a single recipient genetic background with experimental diabetes rather than spontaneous diabetes. Conditioning efficacy and transplantation outcomes could vary with different strain combinations or with autoimmunity. Our findings with preserved fertility are preliminary; the breeder cohort was small and limited to male chimeras. We also did not perform any histology on gonads or other assays to quantify effects of conditioning and fertility preservation. Our data on host and donor immune cell populations that may be responsible for transplant tolerance are based on prior studies that established roles for these cell types, but we did not perform experiments to confirm the same mechanisms in our model. Interrogation of peripheral tolerance in our model remains a challenge given the establishment of central tolerance mechanisms and no prior donor sensitization. Moreover, we assessed peripheral regulatory cells in spleen but not in lymph nodes draining the transplantation site.

STAR★METHODS

RESOURCE AVAILABILITY

Lead contact—Further information and requests for resources and reagents should be directed to and will be fulfilled by the lead contact, Seung Kim (seungkim@stanford.edu).

Materials availability—This study did not generate new unique animals or reagents.

Data and code availability

- All data reported in this paper will be shared by the lead contact upon request.
- This paper does not report original code.

- Any additional information required to reanalyze the data reported in this paper is available from the lead contact upon request.

EXPERIMENTAL MODEL AND SUBJECT DETAILS

Female and male B6 CD45.1 (Stock #: 002014), BALB/c (Stock #: 000651), and FVB (Stock #: 001800) mice 7–8 weeks old were purchased from The Jackson Laboratory (Bar Harbor, ME). B6 RIP-DTR mice were generated and maintained by our group (Bhagchandani et al., 2022). Males were used at 16–20 weeks old, and females were used at 8–10 weeks old. This strain expresses the *Ins2-HBEGF* (RIP-DTR) transgene and the mutant $Ptprc^a$ (CD45.1) allele on the B6 mouse background. The RIP-DTR transgene allows for rapid induction of diabetes by β-cell-specific ablation with 100% penetrance by a single i.p. injection of diphtheria toxin in males and females. Healthy euglycemic littermates of the same sex were randomly assigned to experimental groups and were not involved in any prior procedures. All animals were fed standard chow and water ad *libitum* and housed in non-specific-pathogen-free conditions at the Stanford School of Medicine. Animal experiments were approved by the Stanford Administrative Panel on Laboratory Animal Care.

METHOD DETAILS

Conditioning, reagents, and equipment—A graphical timeline of conditioning is shown in Figure 1B. Mice were given 500μg diphenhydramine HCl i.p. approximately 10–15 min prior to αCD117. 500μg αCD117 was injected retro-orbitally into mice under isoflurane anesthesia on day −6 prior to HCT. Mice were irradiated on day −3 with 200 cGy (Figures 1 and 2) or 300 cGy (Figures 3 and 4) TBI. 300μg each of αCD4 and αCD8 was administered i.p. on days −2, −1, and 0. αCD117 mAb, ACK2 was purchased from Bio X Cell (Lebanon, NH) or BioLegend (San Diego, CA). αCD4 (GK1.5) and αCD8 (YTS169.4) were purchased from Bio X Cell. Diphenhydramine HCl was purchased from MedChem Express (Monmouth Junction, NJ).

Animal irradiation (XRT) was performed using a Kimtron Polaris IC-250 Biological Irradiator (Oxford, CT) with a 225 kV X-ray tube filtered by 0.5mm Cu source set at 225kV, 13.3mA. Mice were divided in irradiation pie cages from Braintree Scientific (Braintree, MA) when irradiated. Dosimetry calibration for our setup was performed using published methods on radiochromic film (Ma et al., 2001).

Bone marrow isolation—Sex-matched donor BALB/c mice (6–7 weeks old) were euthanized and femurs, tibias, and vertebral bodies were collected. Bones were crushed via mortar and pestle in PBS with 2% FBS and 10mM HEPES to recover WBM. WBM was filtered through a 70-μm cell strainer and RBCs were lysed in RBC Lysis Buffer (BioLegend) then manually counted via staining by Trypan Blue (StemCell Technologies).

HSPC enrichment and transplant—Lineage-negative (Lin^-) bone marrow cells were prepared by magnetic column separation using a Lineage Cell Depletion cocktail (Miltenyi Biotec) as per manufacturer's instructions. To further purify the cells collected in the flow through from magnetic separation, Lin^-cKit^+ (LK) cells were sorted as described in flow

cytometry methods. Mice were anesthetized with isoflurane and given retroorbital injections of 1.5E6 LK cells suspended in 100 μL of PBS. Typical HSPC preparation composition can be seen in Figure S6.

Islet isolation and transplantation—Islet isolation and transplantation was performed as previously described with minor modifications (Chang et al., 2018a, 2018b). Briefly, pancreases are perfused with 100–125μg/mL Liberase TL (Roche Diagnostics, Indianapolis, IN) and digested in a 37°C water bath for 18–22 min. After washing with Hank's Buffered Saline (HBS; Caisson Labs, Smithfield, UT), the crude digest is purified over a discontinuous density gradient, washed once more with HBS, and cultured overnight in RPMI 1640 (Corning; Corning NY) supplemented with 10% FBS, 10mM HEPES, and 1% penicillin-streptomycin solution. Recipient mice are anesthetized with ketamine and xylazine and given subcutaneous analgesics. After overnight culture, 100–400 islets are loaded into polyethylene (PE)-50 tubing (BD, Franklin Lakes, NJ) and injected under the kidney capsule of recipient mice. Diabetic mice may be temporarily treated with insulin implants (Linshin, Toronto, Ontario) and/or insulin glargine (Sanofi, Bridgewater, NJ) as indicated in the text and Figure Legends.

Histology—Islet graft-bearing kidneys, pancreases, and intestines fixed in 4% paraformaldehyde were embedded in optimal cutting temperature compound and frozen on dry ice. 6–10μm sections were made on a Leica CM3050 S (Leica Biosystems, Buffalo Grove, IL). Immunofluorescent staining was performed using standard methods. Briefly, sections were blocked in 5% BSA for 1hr then incubated with primary antibodies overnight at 4°C. Sections are washed 3 × 5 min before incubation with secondary antibodies for 2 hours at room temperature and washed 3 × 5 min again. Slide covers were secured with Hard-set Mounting Medium with DAPI (Santa Cruz Biotechnology, Dallas TX). Slides were imaged on an EVOS M5000 Cell Imaging System (ThermoFisher). Post-processing and color channel merging was performed in Fiji (http://fiji.sc/) (Schindelin et al., 2012). Primary antibodies (1:100–200): αCD3 (17A2) and αCD45 (30-F11) were purchased from BioLegend, insulin (a0564) from Dako (Carpinteria, CA). Secondary antibodies (1:200–500): CF-594 and CF-488A α-Guinea Pig were purchased from MilliporeSigma (St. Louis, MO), Alexa Fluor-594 and Alexa Fluor-488 α-Rat, and Alexa Fluor-594 α-Rabbit were purchased from BioLegend.

Peripheral blood, spleen, thymus, and BM preparation for flow cytometry—100 μL of whole blood was collected via the tail vain into EDTA coated tubes. Spleens and thymuses were directly mashed through a 70μm cell strainer. BM cells were isolated as above. Samples underwent RBC lysis in RBC Lysis Buffer (BioLegend) before down-stream staining for analysis.

Flow cytometry analysis—Gating strategies can be found in Supplemental Information (Figures S7 and S8). For analysis of mixed chimerism, cells were first stained with LIVE/DEAD Fixable Near-IR Dead Cell Stain Kit (ThermoFisher Scientific) and blocked with TruStain FcX anti-mouse (Biolegend) for 10 min on ice in Cell Stain Buffer (Biolegend). Antibodies used for staining from Biolegend were as follows: CD45.1 PerCp-Cy5.5 (A20),

CD45.2 Pacific Blue (104), CD3 AF488 (17A2), CD4 PE (RM4–4), CD11b BV605 (M1/70), CD19 PE-Cy7 (6D5), CD49b APC (DX5), CD25 PE-Cy5 (PC61), CD8a PE (53–6.7), Ter-119 PE, CD11b PE (M1/70), Gr-1 PE (RB6–8C5), CD3 PE (17A2), B220 PE (RA3–6B2), CD317 PE (927), CD172a APC (P84), CD11c AF700 (N418), CD304 PE (3E12), FOXP3 AF647 (150D), Helios AF488 (22F6), B220 FITC (RA3–6B2), CD8a BV510 (53–6.7). eBioscience antibodies used were as follows: CD117 APC (2B8), Sca-1 Pe-Cy7 (D7). Staining of intracellular markers was conducted with Biolegend True-Nuclear Transcription Factor Buffer Set as per manufacturer's instructions. For live cell sorting, propidium iodide (MilliporeSigma) was used to determine viability. Cells were analyzed and/or sorted with a BD FACSAria II. Data were analyzed using FlowJo (10.7).

QUANTIFICATION AND STATISTICAL ANALYSIS

Statistical details of all experiments can be found in the figure legends and results section, including value of n. All data are presented as means ± SEM, where n represents number of animals. Animals were randomly assigned to experimental groups and all samples represent biological replicates. Statistical analysis was performed using Prism 8 (GraphPad, San Diego, CA). Differences between the means of two groups were tested using unpaired two-tailed Student's *t*-test with Welch's correction. Some data were excluded by Prism 8's outlier function. Sample size estimates were not used. A p value of 0.05 or less was considered statistically significant. *$p < 0.05$, **$p < 0.01$.

Supplementary Material

Refer to Web version on PubMed Central for supplementary material.

ACKNOWLEDGMENTS

We thank Drs. R. Whitener for advice regarding flow cytometry, K. Jensen and B. Iliopoulou for advice on experimental design, E. Graves for assistance with TBI, and K. Loh for encouragement. Visual abstract created with BioRender (https://biorender.com/). C.A.C. was supported by a Stanford Maternal and Child Health Research Institute fellowship. P.B. is a student in the Medical Scientist Training Program (T32 GM736543) and the Immunology program at Stanford. E.M. was supported by a JDRF Career Development Award. Work in the Kim group was supported by awards from the JDRF (Northern California Center of Excellence), NIH (R01 DK107507; R01 DK108817; U01 DK123743; and P30 DK116074 to S.K.K.), the H.L. Snyder Foundation, gifts from the Reid family, the Skeff family, and by the Stanford Diabetes Research Center Islet Core.

REFERENCES

Adeegbe D, Levy RB, and Malek TR (2010). Allogeneic T regulatory cell-mediated transplantation tolerance in adoptive therapy depends on dominant peripheral suppression and central tolerance. Blood 115, 1932–1940. 10.1182/blood-2009-08-238584. [PubMed: 20040758]

Agarwal R, Dvorak CC, Prockop S, Kwon H-S, Long-Boyle JR, Le A, Brown JW, Merkel E, Truong K, Velasco B, et al. (2021). JSP191 as a single-agent conditioning regimen results in successful engraftment, donor myeloid chimerism, and production of donor derived naïve lymphocytes in patients with severe combined immunodeficiency (SCID). Blood 138, 554. 10.1182/blood-2021-153074.

Aoki H, Hara A, Motohashi T, and Kunisada T (2011). Protective effect of Kit signaling for melanocyte stem cells against radiation-induced genotoxic stress. J. Invest. Dermatol 131, 1906–1915. 10.1038/jid.2011.148. [PubMed: 21633369]

Aoki H, Hara A, Motohashi T, and Kunisada T (2013). Keratinocyte stem cells but not melanocyte stem cells are the primary target for radiation-induced hair graying. J. Invest. Dermatol 133, 2143–2151. 10.1038/jid.2013.155. [PubMed: 23549419]

Audiger C, Rahman MJ, Yun TJ, Tarbell KV, and Lesage S (2017). The importance of dendritic cells in maintaining immune tolerance. J. Immunol 198, 2223–2231. 10.4049/jimmunol.1601629. [PubMed: 28264998]

Baba T, Nakamoto Y, and Mukaida N (2009). Crucial contribution of thymic Sirp alpha+ conventional dendritic cells to central tolerance against blood-borne antigens in a CCR2-dependent manner. J. Immunol 183, 3053–3063. 10.4049/jimmunol.0900438. [PubMed: 19675159]

Bacigalupo A, Ballen K, Rizzo D, Giralt S, Lazarus H, Ho V, Apperley J, Slavin S, Pasquini M, Sandmaier BM, et al. (2009). Defining the intensity of conditioning regimens: working definitions. Biol. Blood Marrow Transplant 15, 1628–1633. 10.1016/j.bbmt.2009.07.004. [PubMed: 19896087]

Bartlett ST, Markmann JF, Johnson P, Korsgren O, Hering BJ, Scharp D, Kay TWH, Bromberg J, Odorico JS, Weir GC, et al. (2016). Report from IPITA-TTS opinion leaders meeting on the future of beta-cell replacement. Transplantation 100 (Suppl 2), S1–S44. 10.1097/TP.0000000000001055.

Beilhack GF, Scheffold YC, Weissman IL, Taylor C, Jerabek L, Burge MJ, Masek MA, and Shizuru JA (2003). Purified allogeneic hematopoietic stem cell transplantation blocks diabetes pathogenesis in NOD mice. Diabetes 52, 59–68. 10.2337/diabetes.52.1.59. [PubMed: 12502494]

Bhagchandani P, Chang CA, Zhao W, Ghila L, Herrera PL, Chera S, and Kim SK (2022). Islet cell replacement and transplantation immunology in a mouse strain with inducible diabetes. Sci. Rep 12, 9033. 10.1038/s41598-022-13087-3. [PubMed: 35641781]

Borgström B, Fridströ m M, Gustafsson B, Ljungman P, and Rodriguez-Wallberg KA (2020). A prospective study on the long-term outcome of prepubertal and pubertal boys undergoing testicular biopsy for fertility preservation prior to hematologic stem cell transplantation. Pediatr. Blood Cancer 67, e28507. 10.1002/pbc.28507.

Busque S, Scandling JD, Lowsky R, Shizuru J, Jensen K, Waters J, Wu HH, Sheehan K, Shori A, Choi O, et al. (2020). Mixed chimerism and acceptance of kidney transplants after immunosuppressive drug withdrawal. Sci. Transl. Med 12, eaax8863. 10.1126/scitranslmed.aax8863.

Chang CA, Akinbobuyi B, Quintana JM, Yoshimatsu G, Naziruddin B, and Kane RR (2018a). Ex-vivo generation of drug-eluting islets improves transplant outcomes by inhibiting TLR4-Mediated NFkB upregulation. Biomaterials 159, 13–24. 10.1016/j.biomaterials.2017.12.020. [PubMed: 29309990]

Chang CA, Murphy K, Kane RR, Lawrence MC, and Naziruddin B (2018b). Early TLR4 blockade attenuates sterile inflammation-mediated stress in islets during isolation and promotes successful transplant outcomes. Transplantation 102, 1505–1513. 10.1097/TP.0000000000002287. [PubMed: 29787520]

Chen YB, Efebera YA, Johnston L, Ball ED, Avigan D, Lekakis LJ, Bachier CR, Martin P, Duramad O, Ishii Y, et al. (2017). Increased Foxp3(+)Helios(+) regulatory T cells and decreased acute graft-versus-host disease after allogeneic bone marrow transplantation in patients receiving sirolimus and RGI-2001, an activator of invariant natural killer T cells. Biol. Blood Marrow Transplant 23, 625–634. 10.1016/j.bbmt.2017.01.069. [PubMed: 28104514]

Chhabra A, Ring AM, Weiskopf K, Schnorr PJ, Gordon S, Le AC, Kwon HS, Ring NG, Volkmer J, Ho PY, et al. (2016). Hematopoietic stem cell transplantation in immunocompetent hosts without radiation or chemotherapy. Sci. Transl. Med 8, 351ra105. 10.1126/scitranslmed.aae0501.

Couto-Silva AC, Trivin C, Thibaud E, Esperou H, Michon J, and Brauner R (2001). Factors affecting gonadal function after bone marrow transplantation during childhood. Bone Marrow Transplant. 28, 67–75. 10.1038/sj.bmt.1703089. [PubMed: 11498747]

Czechowicz A, Kraft D, Weissman IL, and Bhattacharya D (2007). Efficient transplantation via antibody-based clearance of hematopoietic stem cell niches. Science 318, 1296–1299. 10.1126/science.1149726. [PubMed: 18033883]

Czerw T, Labopin M, Schmid C, Cornelissen JJ, Chevallier P, Blaise D, Kuball J, Vigouroux S, Garban F, Lioure B, et al. (2016). High CD3+ and CD34+ peripheral blood stem cell grafts content is associated with increased risk of graft-versus-host disease without beneficial effect on disease control after reduced-intensity conditioning allogeneic transplantation from matched unrelated donors for acute myeloid leukemia - an analysis from the Acute Leukemia Working Party of the

European Society for Blood and Marrow Transplantation. Oncotarget 7, 27255–27266. 10.18632/oncotarget.8463. [PubMed: 27036034]

Finke J, and Mertelsmann R (2015). Use of recombinant growth factors after hematopoietic cell transplantation. In Thomas' Hematopoietic Cell Transplantation, pp. 480–491. 10.1002/9781118416426.ch43.

Fishman JA (2017). Infection in organ transplantation. Am. J. Transplant 17, 856–879. 10.1111/ajt.14208. [PubMed: 28117944]

Flowers MED, and Martin PJ (2015). How we treat chronic graft-versus-host disease. Blood 125, 606–615. 10.1182/blood-2014-08-551994. [PubMed: 25398933]

Hadeiba H, Lahl K, Edalati A, Oderup C, Habtezion A, Pachynski R, Nguyen L, Ghodsi A, Adler S, and Butcher EC (2012). Plasmacytoid dendritic cells transport peripheral antigens to the thymus to promote central tolerance. Immunity 36, 438–450. 10.1016/j.immuni.2012.01.017. [PubMed: 22444632]

Haghiri S, Fayech C, Mansouri I, Dufour C, Pasqualini C, Bolle S, Rivollet S, Dumas A, Boumaraf A, Belhout A, et al. (2021). Long-term follow-up of high-risk neuroblastoma survivors treated with high-dose chemotherapy and stem cell transplantation rescue. Bone Marrow Transplant. 56, 1984–1997. 10.1038/s41409-021-01258-1. [PubMed: 33824435]

Herbin O, Bonito AJ, Jeong S, Weinstein EG, Rahman AH, Xiong H, Merad M, and Alexandropoulos K (2016). Medullary thymic epithelial cells and CD8alpha(+) dendritic cells coordinately regulate central tolerance but CD8alpha(+) cells are dispensable for thymic regulatory T cell production. J. Autoimmun 75, 141–149. 10.1016/j.jaut.2016.08.002. [PubMed: 27543048]

Hering BJ, Clarke WR, Bridges ND, Eggerman TL, Alejandro R, Bellin MD, Chaloner K, Czarniecki CW, Goldstein JS, Hunsicker LG, et al. (2016). Phase 3 trial of transplantation of human islets in type 1 diabetes complicated by severe hypoglycemia. Diabetes Care 39, 1230–1240. 10.2337/dc15-1988. [PubMed: 27208344]

Huang Y, Elliott MJ, Yolcu ES, Miller TO, Ratajczak J, Bozulic LD, Wen Y, Xu H, Ratajczak MZ, and Ildstad ST (2016). Characterization of human CD8(+)TCR(−) facilitating cells *in vitro* and *in vivo* in a NOD/SCID/IL2r-gamma(null) mouse model. Am. J. Transplant 16, 440–453. 10.1111/ajt.13511. [PubMed: 26550777]

Joshi S, Savani BN, Chow EJ, Gilleece MH, Halter J, Jacobsohn DA, Pidala J, Quinn GP, Cahn JY, Jakubowski AA, et al. (2014). Clinical guide to fertility preservation in hematopoietic cell transplant recipients. Bone Marrow Transplant. 49, 477–484. 10.1038/bmt.2013.211. [PubMed: 24419521]

Kawai T, Cosimi AB, Spitzer TR, Tolkoff-Rubin N, Suthanthiran M, Saidman SL, Shaffer J, Preffer FI, Ding R, Sharma V, et al. (2008). HLA-mismatched renal transplantation without maintenance immunosuppression. N. Engl. J. Med 358, 353–361. 10.1056/NEJMoa071074. [PubMed: 18216355]

Klein L, Kyewski B, Allen PM, and Hogquist KA (2014). Positive and negative selection of the T cell repertoire: what thymocytes see (and don't see). Nat. Rev. Immunol 14, 377–391. 10.1038/nri3667. [PubMed: 24830344]

Law CL, and Grewal IS (2009). Therapeutic interventions targeting CD40L (CD154) and CD40: the opportunities and challenges. Adv. Exp. Med. Biol647, 8–36. 10.1007/978-0-387-89520-8_2. [PubMed: 19760064]

Lazaryan A, Weisdorf DJ, DeFor T, Brunstein CG, MacMillan ML, Bejanyan N, Holtan S, Blazar BR, Wagner JE, and Arora M (2016). Risk factors for acute and chronic graft-versus-host disease after allogeneic hematopoietic cell transplantation with umbilical cord blood and matched sibling donors. Biol. Blood Marrow Transplant 22, 134–140. 10.1016/j.bbmt.2015.09.008. [PubMed: 26365153]

Lecker J, and Froberg-Fejko K (2016). Using environmental enrichment and nutritional supplementation to improve breeding success in rodents. Lab Anim. 45, 406–407. 10.1038/laban.1114.

Lee JH, Joo YD, Kim H, Ryoo HM, Kim MK, Lee GW, Lee JH, Lee WS, Park JH, Bae SH, et al. (2013). Randomized trial of myeloablative conditioning regimens: busulfan plus cyclophosphamide versus busulfan plus fludarabine. J. Clin. Oncol 31, 701–709. 10.1200/JCO.2011.40.2362. [PubMed: 23129746]

Leventhal J, Abecassis M, Miller J, Gallon L, Ravindra K, Tollerud DJ, King B, Elliott MJ, Herzig G, Herzig R, and Ildstad ST (2012). Chimerism and tolerance without GVHD or engraf™ent syndrome in HLA-mismatched combined kidney and hematopoietic stem cell transplantation. Sci. Transl. Med 4, 124ra28. 10.1126/scitranslmed.3003509.

Leventhal JR, and Mathew JM (2020). Outstanding questions in transplantation: Tolerance. Am. J. Transplant 20, 348–354. 10.1111/ajt.15680. [PubMed: 31675469]

Luo B, Nanji SA, Schur CD, Pawlick RL, Anderson CC, and Shapiro AMJ (2005). Robust tolerance to fully allogeneic islet transplants achieved by chimerism with minimal conditioning. Transplantation 80, 370–377. 10.1097/01.tp.0000167724.38038.ae. [PubMed: 16082333]

Ma CM, Coffey CW, DeWerd LA, Liu C, Nath R, Seltzer SM, and Seuntjens JP; American Association of Physicists in Medicine (2001). AAPM protocol for 40–300 kV x-ray beam dosimetry in radiotherapy and radio-biology. Med. Phys 28, 868–893. 10.1118/1.1374247. [PubMed: 11439485]

Messner F, Etra JW, Dodd-O JM, and Brandacher G (2019). Chimerism, transplant tolerance, and beyond. Transplantation 103, 1556–1567. 10.1097/TP.0000000000002711. [PubMed: 30896678]

Miranda PM, Mohan V, Ganthimathy S, Anjana RM, Gunasekaran S, Thiagarajan V, Churchill TA, Kin T, Shapiro AMJ, and Lakey JRT (2013). Human islet mass, morphology, and survival after cryopreservation using the Edmonton protocol. Islets 5, 188–195. 10.4161/isl.26304. [PubMed: 24759005]

Nakasone H, Fukuda T, Kanda J, Mori T, Yano S, Kobayashi T, Miyamura K, Eto T, Kanamori H, Iwato K, et al. (2015). Impact of conditioning intensity and TBI on acute GVHD after hematopoietic cell transplantation. Bone Marrow Transplant. 50, 559–565. 10.1038/bmt.2014.293. [PubMed: 25531281]

Nikolic B, Onoe T, Takeuchi Y, Khalpey Z, Primo V, Leykin I, Smith RN, and Sykes M (2010). Distinct requirements for achievement of allotolerance versus reversal of autoimmunity via nonmyeloablative mixed chimerism induction in NOD mice. Transplantation 89, 23–32. 10.1097/TP.0b013e3181c4692e. [PubMed: 20061915]

Nikolic B, Takeuchi Y, Leykin I, Fudaba Y, Smith RN, and Sykes M (2004). Mixed hematopoietic chimerism allows cure of autoimmune diabetes through allogeneic tolerance and reversal of autoimmunity. Diabetes 53, 376–383. 10.2337/diabetes.53.2.376. [PubMed: 14747288]

Pathak S, and Meyer EH (2020). Tregs and mixed chimerism as approaches for tolerance induction in islet transplantation. Front. Immunol 11, 612737. 10.3389/fimmu.2020.612737.

Persaud SP, Ritchey JK, Kim S, Lim S, Ruminski PG, Cooper ML, Rettig MP, Choi J, and DiPersio JF (2021). Antibody-drug conjugates plus Janus kinase inhibitors enable MHC-mismatched allogeneic hematopoietic stem cell transplantation. J. Clin. Invest 131, e145501. 10.1172/JCI145501.

Pullen LC (2021). Islet cell transplantation hits a milestone. Am. J. Transplant 21, 2625–2626. 10.1111/ajt.16039. [PubMed: 34352933]

Rickert CG, and Markmann JF (2019). Current state of organ transplant tolerance. Curr. Opin. Organ Transplant 24, 441–450. 10.1097/MOT.0000000000000670. [PubMed: 31169530]

Rogers NM, Isenberg JS, and Thomson AW (2013). Plasmacytoid dendritic cells: no longer an enigma and now key to transplant tolerance? Am. J.Transplant 13, 1125–1133. 10.1111/ajt.12229. [PubMed: 23617754]

Schindelin J, Arganda-Carreras I, Frise E, Kaynig V, Longair M, Pietzsch T, Preibisch S, Rueden C, Saalfeld S, Schmid B, et al. (2012). Fiji: an open-source platform for biological-image analysis. Nat. Methods 9, 676–682. 10.1038/nmeth.2019. [PubMed: 22743772]

Shaw P, Shizuru J, Hoenig M, Veys P, and Iewp E (2019). Conditioning perspectives for primary immunodeficiency stem cell transplants. Front. Pediatr 7, 434. 10.3389/fped.2019.00434. [PubMed: 31781522]

Wang M, Racine J, Zhang M, Wu T, Deng R, Johnston H, Shen C, Siswanto K, and Zeng D (2014). MHC-mismatched chimerism is required for induction of transplantation tolerance in autoimmune nonobese diabetic recipients. J. Immunol 193, 2005–2015. 10.4049/jimmunol.1401137. [PubMed: 25000982]

Wikander I, Lundberg FE, Nilsson H, Borgströ m B, and Rodriguez-Wall-berg KA (2021). A prospective study on fertility preservation in prepubertal and adolescent girls undergoing hematological stem cell transplantation. Front. Oncol 11, 692834. 10.3389/fonc.2021.692834.

Xu H, Zhu Z, Huang Y, Bozulic LD, Hussain LR, Yan J, and Ildstad ST (2012). Innate and adaptive immune responses are tolerized in chimeras prepared with nonmyeloablative conditioning. Transplantation 93, 469–476. 10.1097/TP.0b013e318242bddf. [PubMed: 22228418]

Xue X, Pech NK, Shelley WC, Srour EF, Yoder MC, and Dinauer MC (2010). Antibody targeting KIT as pretransplantation conditioning in immunocompetent mice. Blood 116, 5419–5422. 10.1182/blood-2010-07-295949. [PubMed: 20813896]

Yadav M, Stephan S, and Bluestone JA (2013). Peripherally induced tregs - role in immune homeostasis and autoimmunity. Front. Immunol 4, 232. 10.3389/fimmu.2013.00232. [PubMed: 23966994]

Zirpel H, and Roep BO (2021). Islet-resident dendritic cells and macrophages in type 1 diabetes: in search of bigfoot's print. Front. Endocrinol 12, 666795. 10.3389/fendo.2021.666795.

Zuber J, and Sykes M (2017). Mechanisms of mixed chimerism-based transplant tolerance. Trends Immunol. 38, 829–843. 10.1016/j.it.2017.07.008. [PubMed: 28826941]

Highlights

- Stable mixed hematopoietic chimerism achieved without myeloablative conditioning
- Chimerism confers allotolerance to MHC-mismatched islets without immunosuppression
- Simultaneous hematopoietic cell and islet transplantation durably corrects diabetes
- Central and peripheral tolerance mechanisms likely mediate islet allotolerance

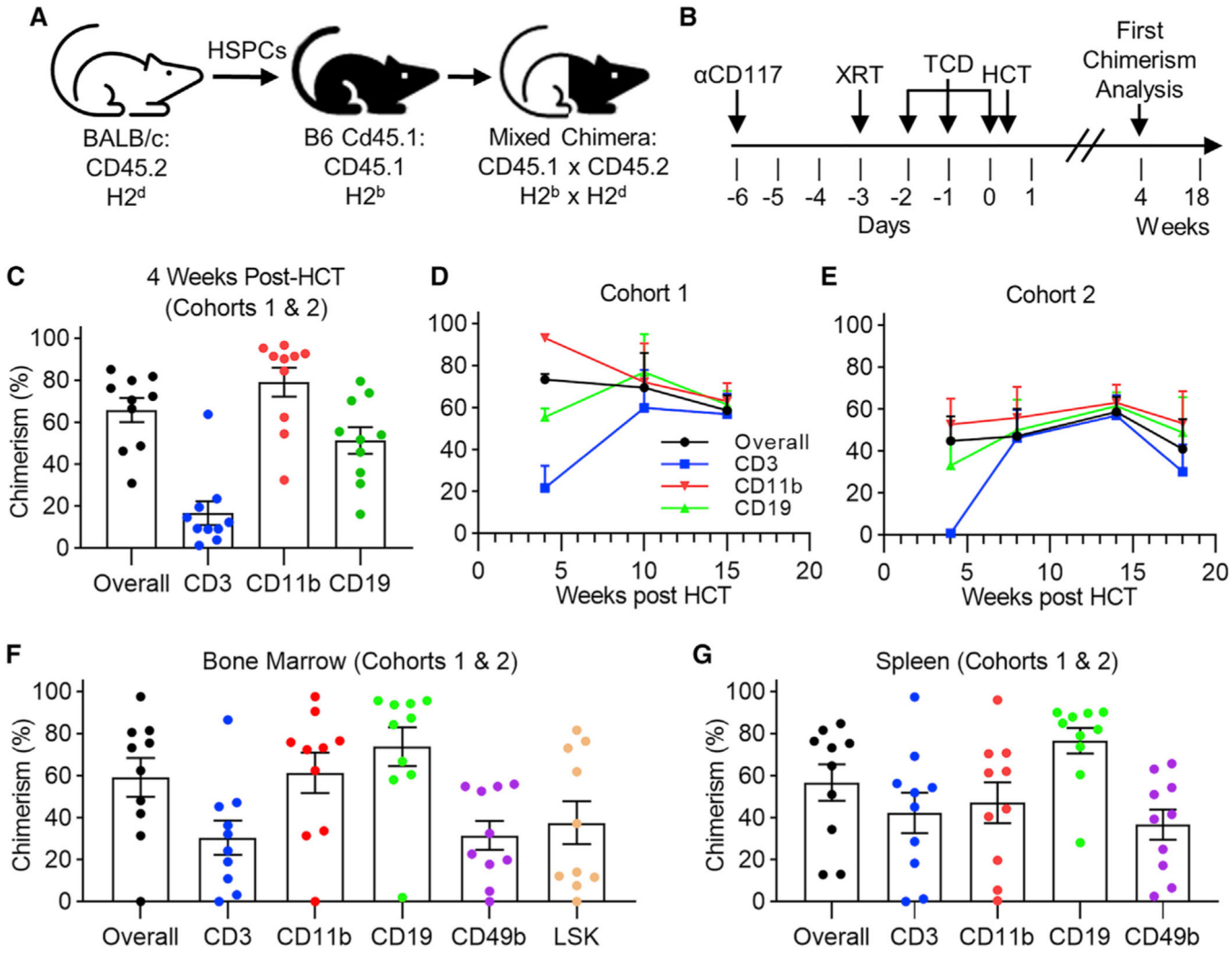

Figure 1. Non-myeloablative conditioning promotes durable donor chimerism across fully mismatched MHC barriers

(A) Transplantation model and strains used.

(B) Reduced intensity conditioning regimen. 500 ug αCD117 is administered on day −6, then 200 cGy XRT on day −3, then 300 ug of αCD4/CD8 each on days −2 through 0. On day 0, mice are transplanted with 1.5E6 $Lin^{-}cKit^{+}$ HSPCs after the final TCD treatment.

(C) Chimerism analysis of peripheral blood 4 weeks after conditioning and HCT including overall chimerism, $CD3^{+}$ T cells, $CD11b^{+}$ myeloid cells, and $CD19^{+}$ B cells.

(D and E) Longitudinal chimerism analysis of peripheral blood in 2 separate experimental cohorts. (D: cohort 1; E: cohort 2; n = 5 per cohort)

(F) Chimerism analysis of recipient bone marrow at 15 or 18 weeks post-HCT including $CD49b^{+}$ NK cells and $Lin^{-}Sca1^{+}cKit^{+}$ (LSK) cells.

(G) Chimerism analysis of recipient spleen at 15 or 18 weeks post-HCT (n = 10, sum of 2 independent experiments). HSPCs, hematopoietic stem and progenitor cells; XRT, X-ray therapy; TCD, T cell depletion; HCT, hematopoietic cell transplant. X-ray therapy; TCD, T cell depletion; HCT, hematopoietic cell transplant.

(C–G) Data show mean ± SEM.

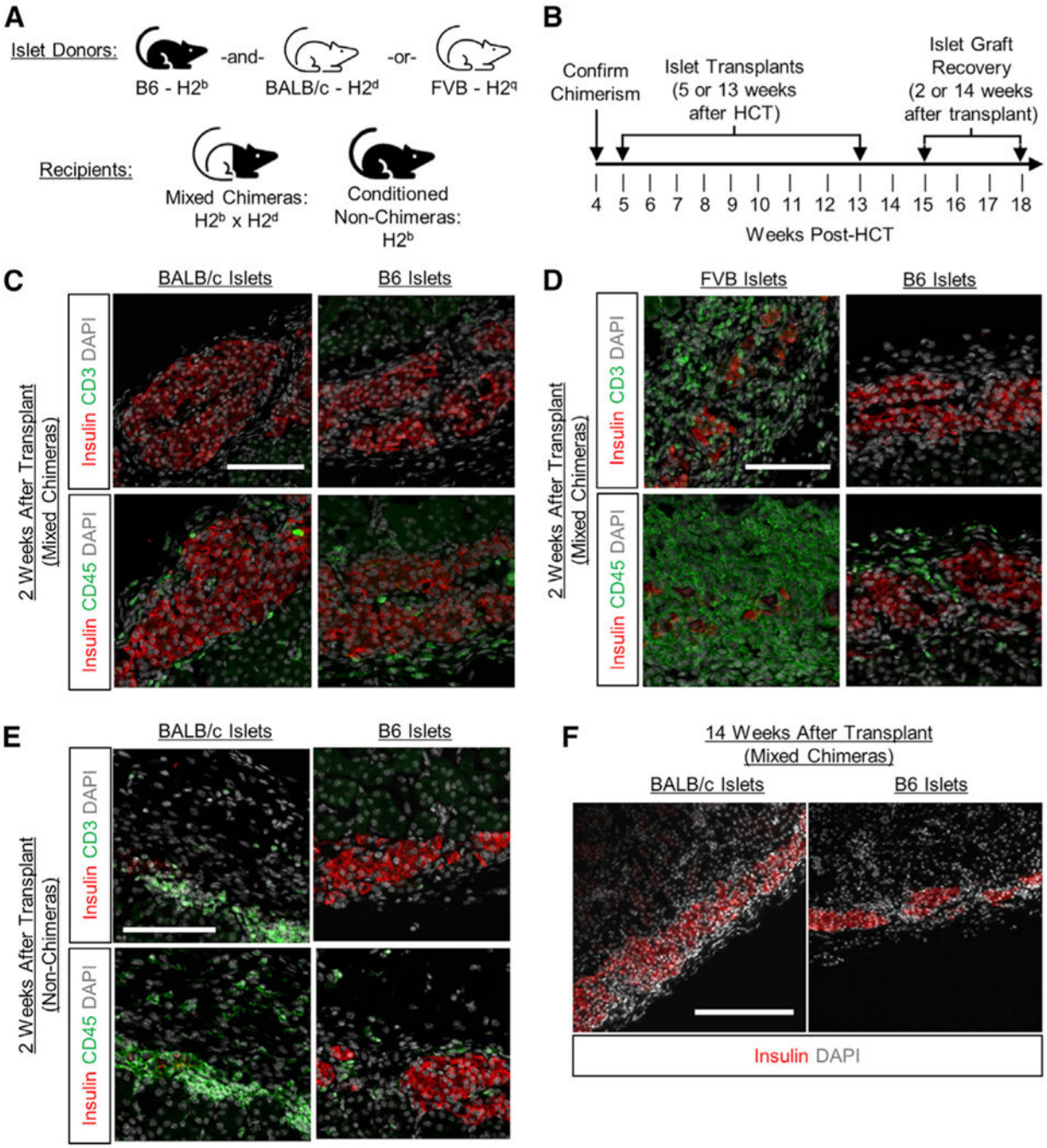

Figure 2. Histology of short- and long-term islet transplants in mixed chimeras

(A) Experimental transplantation schematic. Mixed chimeras received B6 islets in the left kidney and BALB/c (n = 7) or FVB (n = 3) islets in the opposite kidney. Conditioned non-chimeras received B6 islets in the left kidney and BALB/c islets in the opposite kidney (n = 3).

(B) Experimental timeline for islet transplants. Some islet grafts transplanted in mice 13 weeks post-HCT were recovered after 2 weeks (short-term). Other islet grafts (long-term)

transplanted in mice 5 weeks post-HCT were recovered after 14 weeks. Chimerism was verified at 4 weeks post-HCT.

(C) Representative BALB/c and B6 islet grafts 2 weeks after islet transplantation in mixed chimeras stained for insulin and CD3 or CD45 (n = 2).

(D) Representative FVB and B6 islet grafts 2 weeks after islet transplantation in mixed chimeras stained for insulin and CD3 or CD45 (n = 3).

(E) Representative BALB/c and B6 islet grafts 2 weeks after islet transplantation in conditioned non-chimeras stained for insulin and CD3 or CD45 (n = 3).

(F) Representative BALB/c and B6 islet grafts 13 weeks after islet transplantation in mixed chimeras stained for insulin (n = 5).

Scale bars: 100 μm for (C)–(E) and 200 μm for (F).

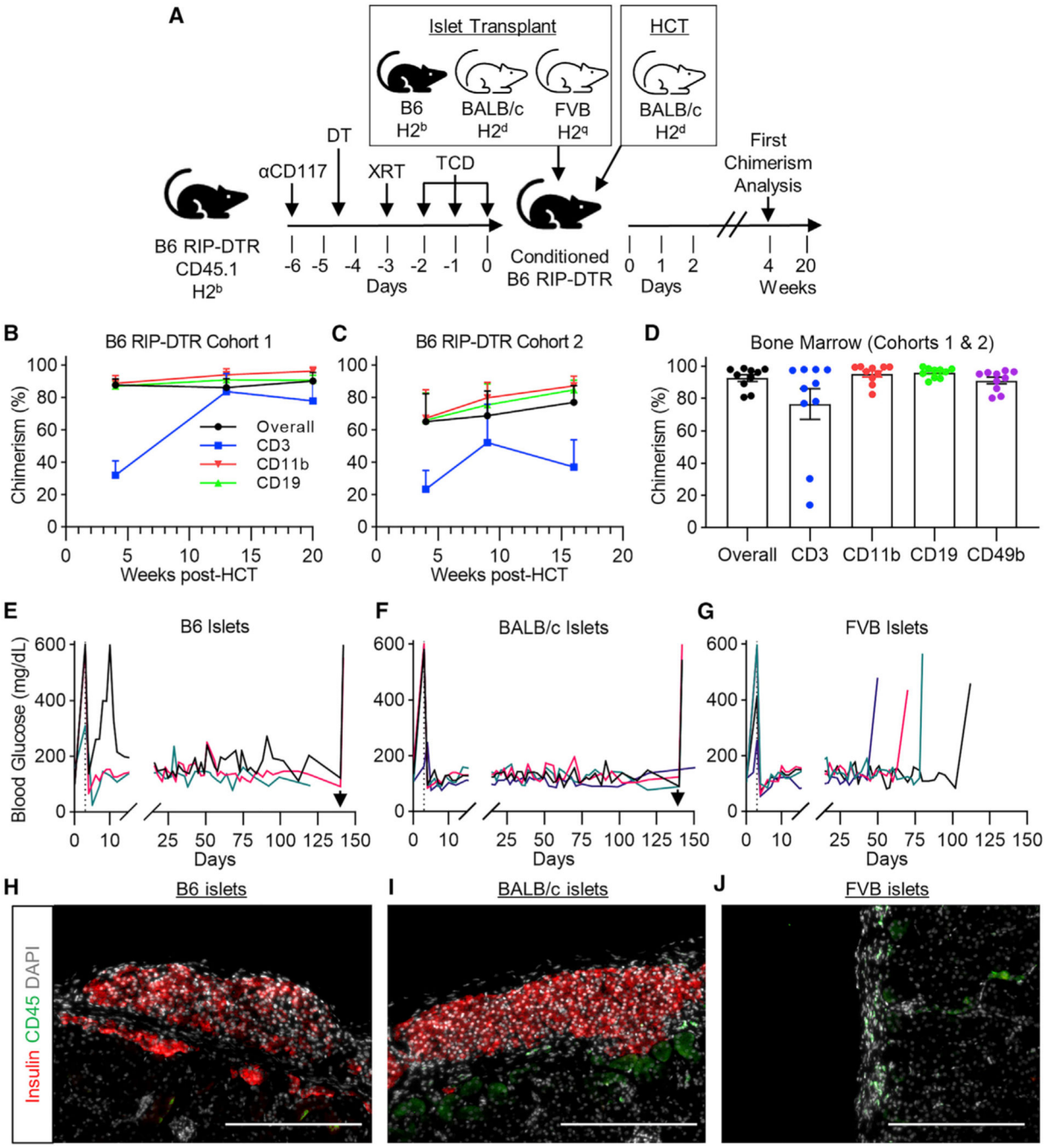

Figure 3. Mixed chimerism in diabetic B6 RIPDTR mice results in long-term, donor-matched islet graft tolerance and diabetes reversal

(A) Experimental conditioning and transplantation outline. Conditioning was initiated on day −6 with αCD117, and diabetes was induced on day −4.5 by DT injection. 300 cGy XRT was given on day −3. On day 0 after the final TCD, B6 RIP-DTR mice received islet grafts from B6, BALB/c, or FVB donors. Following islet transplantation, mice receive 1.5E6 $Lin^{-}cKit^{+}$ HSPCs from BALB/c donors.

(B and C) Longitudinal chimerism analysis demonstrating robust multi-lineage chimerism up to 20 weeks after HCT (B: n = 7 males) or up to 16 weeks after HCT (C: n = 4 females).

(D) Chimerism of different cell subtypes in mixed chimera bone marrow at 16 or 20 weeks after HCT.
(E) Non-fasting blood glucose of mice that received B6 islets. One mouse transiently required insulin after islet transplantation but eventually became insulinin dependent (black line). Vertical dotted line denotes islet transplant and HCT. Arrow indicates nephrectomy in 2 of 3 mice.
(F) Non-fasting blood glucose of mice that received BALB/c islets. Arrow indicates nephrectomy in 3 of 4 mice.
(G) Non-fasting blood glucose of mice that received FVB islets (n = 4). Data shown here do not include glycemia measurements after reversion to hyperglycemia.
(H) Representative B6 islet graft stained for insulin and CD45 at 20 weeks after transplantation in a mixed chimeric recipient (n = 3).
(I) Representative BALB/c islet graft 20 weeks after transplantation in a recipient that developed mixed chimerism (n = 4).
(J) Representative FVB islet graft 20 weeks after transplantation in a recipient that developed mixed chimerism (n = 4). Scale bars in (H–J): 200 μm. DT, diphtheria toxin; XRT, X-ray therapy; TCD, T cell depletion; HCT, hematopoietic cell transplant.
(B–D) Data show mean ± SEM.

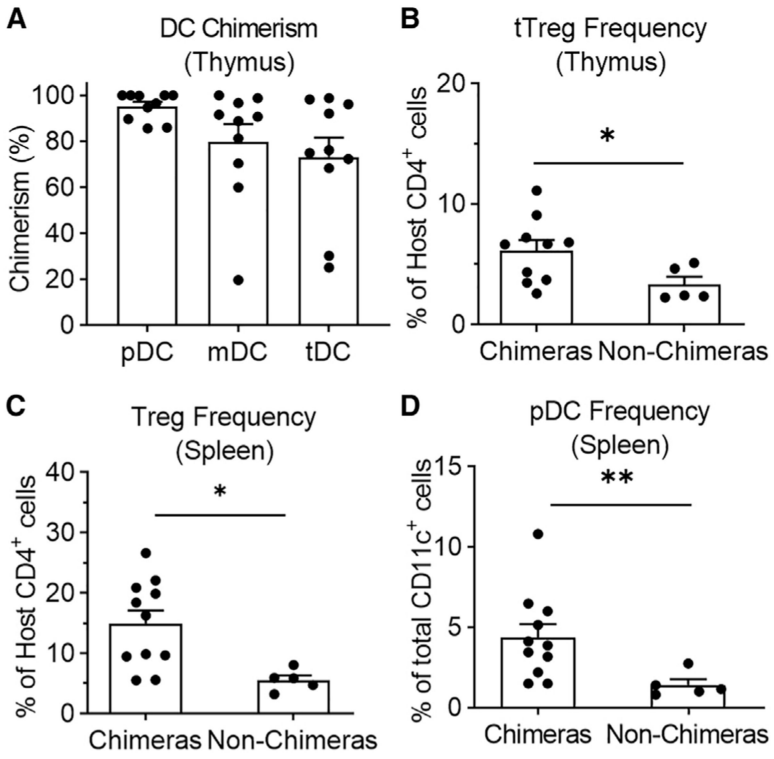

Figure 4. Analysis of cell subsets that modulate central and peripheral tolerance

(A) Chimerism analysis of $CD11c^+$ dendritic cell subsets in the thymus of B6 RIP-DTR mixed chimeras at 16 or 20 weeks post-HCT. pDCs = $B220^+PDCA1^+$, mDC = $B220^-SIRP\alpha^+CD8^-$, tDC = $B220^-SIRP\alpha^-CD8^+$.

(B) Frequency of thymic $CD25^{hi}$ tTregs among host $CD4^+$ T cells in chimeras versus non-chimeras.

(C) Frequency of splenic $CD25^{hi}$ Tregs among host $CD4^+$ T cells in the spleen of chimeras compared with non-chimeras.

(D) Frequency of splenic pDCs among $CD11c^+$ cells in chimeras versus non-chimeras (n = 11 for chimeras and n = 5 for conditioned non-chimeras, sum of 2 experiments).

Data show mean ± SEM. *$p < 0.05$, **$p < 0.01$.

KEY RESOURCES TABLE

REAGENT or RESOURCE	SOURCE	IDENTIFIER
Antibodies		
Goat α-Guinea Pig CF594	MilliporeSigma	Cat#: SAB4600103
Goat α-Guinea Pig CF488A	MilliporeSigma	Cat#: SAB4600040
α-Insulin	Dako	RRID: AB_10013624 Cat#: A0564
α-CD3	Biolegend	RRID: AB_312658 Cat#:100201
α-CD45	Biolegend	RRID: AB_312966 Cat#: 103101
Mouse α-Rat AF488	Biolegend	RRID: AB_2910464 Cat#: 407513
Mouse α-Rat AF594	Biolegend	RRID: AB_2650845 Cat#: 407509
Mouse α-Rabbit AF594	Biolegend	RRID: AB_2832788 Cat#: 410407
TruStain FcX™ Antibody	Biolegend	RRID: AB_1574973 Cat#: 101319
α-CD45.1 PerCp-Cy5.5	Biolegend	RRID: AB_893348 Cat#: 110727
α-CD45.2 Pacific Blue	Biolegend	RRID: AB_492873 Cat#: 109819
α-CD3 AF488	Biolegend	RRID: AB_493530 Cat#: 100212
α-CD4 PE	Biolegend	RRID: AB_313690 Cat#: 116005
α-CD11b BV605	Biolegend	RRID: AB_11126744 Cat#: 101237
α-CD19 PE-Cy7	Biolegend	RRID: AB_313654 Cat#: 115519
α-CD49b APC	Biolegend	RRID: AB_313416 Cat#: 108909
α-CD25 PE-Cy5	Biolegend	RRID: AB_312859 Cat#: 102010
α-CD8a PE	Biolegend	RRID: AB_312746 Cat#; 100707

REAGENT or RESOURCE	SOURCE	IDENTIFIER
α-Ter-119 PE	Biolegend	RRID: AB_313708 Cat#: 116207
α-CD11b PE	Biolegend	RRID: AB_312790 Cat#: 101207
α-Gr-1 PE	Biolegend	RRID: AB_313372 Cat#: 108407
α-CD3 PE	Biolegend	RRID: AB_312662 Cat#: 100205
α-B220 PE	Biolegend	RRID: AB_312992 Cat#: 103207
α-CD317 PE	Biolegend	RRID: AB_1953284 Cat#: 127009
α-CD172a APC	Biolegend	RRID: AB_2564060 Cat#: 144013
α-CD11c AF700	Biolegend	RRID: AB_528735 Cat#: 117319
α-CD304 PE	Biolegend	RRID: AB_2561927 Cat#: 145203
a-FOXP3 AF647	Biolegend	RRID: AB_439749 Cat#: 320013
α-Helios AF488	Biolegend	RRID: AB_10645334 Cat#: 137213
α-B220 FITC	Biolegend	RRID: AB_312990 Cat#: 103205
α-CD8a BV510	Biolegend	RRID: AB_2561389 Cat#: 100751
α-CD117	Biolegend	RRID: AB_2571993 Cat#: 135132
α-CD117 APC	eBioscience	RRID: AB_469430 Cat#: 17-1171-82
α-Sca-1 PE-Cy7	eBioscience	RRID: AB_469669 Cat#: 25-5981-82
α-CD117	BioXCell	Cat#: BE0293
α-CD4	BioXCell	Cat#: BE0003-1
α-CD8	BioXCell	Cat#: BE0117
Chemicals, peptides and recombinant proteins		
LIVE/DEAD™ Fixable Near-IR Dead Cell Stain Kit	ThermoFisher	Cat#: L34975

REAGENT or RESOURCE	SOURCE	IDENTIFIER
Bovine Serum Albumin	Fisher Scientific	Cat#: BP1600-100
RBC Lysis Buffer (10X)	Biolegend	Cat#: 420301
Cell Staining Buffer	Biolegend	Cat#: 420201
True-Nuclear™ Transcription Factor Buffer Set	Biolegend	Cat#: 424401
Propidium Iodide	MilliporeSigma	Cat#: P4170
Liberase™ TL Research Grade	MilliporeSigma	Cat#: 05401020001
Diphenhydramine HCl	Cayman Chemical Company	Cat#:11158
Lineage Cell Depletion Kit, mouse	Miltenyi Biotec	Cat#:130-090-858
HBS	Caisson Labs	Cat#: HBL06
HEPES Solution	Caisson Labs	Cat#: HOL06
RPMI 1640	Corning	Cat#: 10-040-CV
LinBit	LinShin Canada, Inc	Cat#: Pr-1-B
LANTUS®	sanofi-aventis U.S. LLC	NDC 0088–2220-33
UltraCruz® Hard-set Mounting Medium	Santa Cruz Biotechnology	Cat#: sc-359850
Fetal Bovine Serum	Cytiva	Cat#: SH30070.03
Penicillin-Streptomycin	Gibco	Cat#: 15140122
Experimental models: Organisms/strains		
B6 CD45.1 mice	The Jackson Laboratory	Stock #: 002014
BALB/c mice	The Jackson Laboratory	Stock #: 000651
FVB mice	The Jackson Laboratory	Stock #: 001800
B6 *RIP-DTR* mice	Seung Kim Lab, Stanford University	N/A
Software and algorithms		
FlowJo 10.7	FlowJo, LLC	N/A
GraphPad Prism 8	GraphPad Software	N/A
Fiji	Schindelin et al. (2012)	N/A
Other		
IC-250 X-Ray Biological Irradiator System	KIMTRON Inc	N/A
CM3050 S	Leica Biosystems	N/A

REAGENT or RESOURCE	SOURCE	IDENTIFIER
FACS Aria II	BD	N/A
EVOS M5000 Cell Imaging System	ThermoScientific	N/A